ELSEVIER

Surface Science 330 (1995) 86–100

surface science

On the Doyle–Turner representation of the optical potential for RHEED calculations

S.L. Dudarev [a,*], L.-M. Peng [b], M.J. Whelan [a]

[a] *Department of Materials, University of Oxford, Parks Road, Oxford OX1 3PH, UK*

[b] *Beijing Laboratory of Electron Microscopy, Chinese Academy of Sciences, P.O. Box 2724, Beijing 100080, People's Republic of China*

Received 2 January 1995; accepted for publication 15 March 1995

Abstract

The approximate representation of the atomic potential in the form of a set of Gaussian exponential terms has long been recognized as the most convenient method for carrying out many-beam calculations of reflection high-energy electron diffraction (RHEED) intensities. Smith and Burge [Acta Cryst. 15 (1962) 182] and later Doyle and Turner [Acta Cryst. A 24 (1968) 390] (hereafter referred as DT) used Gaussian fitting to represent the scattering factor of a number of elements. However, until recently the coefficients of the DT expansion were only known for the *real* part of the crystal potential. In this paper, we show how the DT parameters can be introduced and calculated for the *imaginary* part of the potential. A set of the DT coefficients is given in tabulated form which provides an accurate approximation to the imaginary part of the potential arising from thermal motion of atoms. These coefficients correspond to the same set of values of the Debye–Waller factor as those used by Radi [Acta Cryst. A26 (1970) 41]. Our analysis shows that in most cases the real space behaviour of the imaginary part of the potential differ substantially from the often assumed hypothesis Im $U(\boldsymbol{r})$ = constant × Re $U(\boldsymbol{r})$, and this difference appears to have a considerable effect on the RHEED intensities calculated using a many-beam approach. Comparison of our calculations with the results obtained recently by other authors suggests that there exist some additional processes of diffuse scattering affecting elastic RHEED intensities. Computer programs used for carrying out calculations of the DT parameters are available upon request.

Keywords: Reflection electron microscopy (REM); Reflection high-energy electron diffraction (RHEED)

1. Introduction

The problem of theoretical calculation of reflection high-energy electron diffraction (RHEED) intensities has attracted considerable attention in recent years. This stems from the fact that although RHEED observations have already provided much of our knowledge about the kinetics of molecular-beam epitaxial growth of many types of materials, the full potential of this electron diffraction technique has yet to be realized. Applications of RHEED rocking curve analysis to the determination of surface structure have recently become available

* Corresponding author. Fax: +44 1865 273764; E-mail: sergei.dudarev@materials.oxford.ac.uk.

0039-6028/95/$09.50
SSDI 0039-6028(95)00464-5

[1–5], and development of a theoretical treatment suitable for multiple scattering calculations of the intensity distribution in the RHEED patterns observed during MBE growth remains the subject of discussions at present [6–8]. Within the framework of a statistical treatment of diffraction of high-energy electrons from partially disordered crystals, the effects of disorder and inelastic scattering lead to an imaginary part of the effective interaction potential entering the Schrödinger equation for the ensemble averaged wave function [9,10]. The imaginary part of the potential gives rise to an effective "absorption" of fast electrons, which, in accordance with the current conservation principle is entirely compensated by a particular term in the kinetic equation for the bilinear combination of wave functions (the so-called density matrix) [8]. Quantitative evaluation of the imaginary part of the potential is therefore required as a starting point of any computational scheme for multiple scattering evaluation of the intensities of Bragg diffraction spots and the cross-section of diffuse scattering.

Among various contributions to the imaginary part of the potential resulting from (i) thermal vibrations of atoms (the so-called TDS scattering), (ii) statistical disorder in atomic arrangement and (iii) electronic excitations [9,10], the first differs from the latter two in that this contribution exists for perfectly ordered surfaces and it affects the intensities of Bragg diffraction spots independently of whether or not energy filtering is employed for carrying out experimental observations [11–13]. The problem of evaluation of the TDS contribution to the imaginary part of the potential has recently been addressed by Bird and King [14] and Weickenmeier and Kohl [15], who developed computer programs suitable for calculation of the imaginary part of the amplitude of scattering of an electron by a single atom in a crystal. These programs evaluate the amplitude of scattering in k-space and are basically designed for applications in transmission high-energy electron diffraction. In the case of RHEED however, the k-space representation of atomic amplitudes appears to be less convenient. This is largely because the projection of the momentum on the surface normal (z-axis) is not conserved (for a recent discussion see Ref. [16]), and numerical computations require application of one of the mixed (k_x, k_y, z)-space approaches [17–27]. The real space variation of the imaginary part of the potential therefore needs to be known, and recently this problem has been dealt with [10,26,28] by carrying out numerical Fourier transformation of the amplitude as calculated using one of the k-space approaches [14,15]. Our experience shows that this method of evaluation of the optical potential in real space, although being rigorous, is relatively time consuming and not very convenient for practical purposes.

The development of computational schemes suitable for carrying out practical RHEED calculations has shown that the most convenient representation of the atomic amplitudes is provided by the Doyle–Turner (DT) form, i.e. by an approximation in which each amplitude is given by a sum of a few Gaussian terms (the idea that the amplitude of scattering can be approximated by a sum of Gaussian terms was initially proposed by Smith and Burge in 1962 [29], but historically it has become usual to name the relevant representation after Doyle and Turner, who published their work [30] six years later). The coefficients of the DT expansion have been tabulated for almost all elements [30,31], and evaluation of the mixed (k_x, k_y, z) representation of the crystal potential using the DT form is about ten times faster than numerical calculation of the Fourier transform of the amplitude. However, in the literature DT coefficients have been tabulated only for the real part of the atomic scattering amplitude, and this has stimulated a widespread use of the so-called "proportional" model in which the imaginary part of the potential is assumed to be proportional to the real part $\mathrm{Im}\, U(\boldsymbol{r}) = \text{constant} \times \mathrm{Re}\, U(\boldsymbol{r})$ (note that that this approximation in fact goes far beyond the original idea of Hashimoto, Howie and Whelan [32] who employed the ratio between the real and imaginary parts *for only a single* Fourier coefficient of the potential). It is well known that this "proportional" model is only a crude first approximation. The phonon imaginary part is known to be more concentrated near the ion cores than the elastic scattering potential [33,34], and there exists experimental evidence obtained by transmission electron diffraction that in some cases the "proportional" model provides a poor description of the observed intensity distributions and more rigorous considerations are required [35,36].

Therefore this shows that the use of the "proportional" model (in which the real part of the potential is given by the DT representation) for carrying out RHEED calculations is basically justified by the convenience of application of the DT approximation for practical calculations and generally the "proportional" model is not

consistent with more rigorous calculations [14,15]. In this paper we discuss how the the advantages of both models can be combined and how the imaginary part of the potential associated with thermal motion of atoms can be represented in the DT form. This appears to be particularly useful for two reasons. Firstly, it is more efficient computationally to have both the real and imaginary parts of the potential represented in a similar form. Secondly, the DT coefficients employed to carry out RHEED calculations for a particular crystal structure can then be *published*, and this enables other researchers to reproduce and verify the relevant numerical results.

Below, we show that in order to introduce the DT representation for the imaginary part of the optical potential it is necessary to modify the definition of the effective atomic amplitude of scattering as compared with the definition given by Bird and King [14]. We find that indeed the behaviour of the imaginary part of the potential in real space deviates considerably from the predictions of the "proportional" model, and propose a practical scheme for evaluation of the relevant DT coefficients. We provide a list of these coefficients calculated for two temperatures (T = 93 K and T = 293 K) and for the same set of the Debye–Waller coefficients as used by Radi [37]. We also analyse how the choice of the imaginary part of the potential affects the results of RHEED intensity calculations. We find that modification of the *shape* of the imaginary part of the potential in real space influences the height of the peaks in the rocking curves, but it does not result in an appreciable shift of the positions of the peaks.

2. The amplitude of scattering

At high energies the matrix element $\langle \boldsymbol{q}|\hat{U}|\boldsymbol{q}'\rangle$ of the effective potential of interaction between the incident electron and a crystal can be written in the form of a superposition of contributions of separate atoms as (see, e.g. Ref. [14])

$$\langle \boldsymbol{q}|\hat{U}|\boldsymbol{q}'\rangle = -\frac{2\pi\hbar^2}{m}\sum_a f_a(\boldsymbol{q},\boldsymbol{q}')\exp[-\mathrm{i}(\boldsymbol{q}-\boldsymbol{q}')\cdot\boldsymbol{R}_a]\exp[-M_a(\boldsymbol{q}-\boldsymbol{q}')], \tag{1}$$

where $f_a(\boldsymbol{q},\boldsymbol{q}')$ is the scattering amplitude of the high-energy electron by an atom in a crystal, m is the electron relativistic mass, $\boldsymbol{R}_a$ denotes the equilibrium position of the nucleus of a particular atom a and $M_a(\boldsymbol{q}) = \frac{1}{2}\langle(\boldsymbol{q}\cdot\boldsymbol{u}_a)^2\rangle$ is the Debye–Waller factor.

Eq. (1) assumes two approximations to be valid. Firstly, representation of the potential of the crystal in terms of a sum of individual contributions of separate atoms neglects the redistribution of charge due to chemical bonding. A detailed discussion of this subject is given in the book [11] where it is shown that chemical bonding affects only the lower-order Fourier components of the potential and generally Eq. (1) is valid within the accuracy of a few percent. Secondly, Eq. (1) is valid provided that the main contribution to the imaginary part of the amplitude $f_a(\boldsymbol{q},\boldsymbol{q}') = f'_a(\boldsymbol{q}-\boldsymbol{q}') + \mathrm{i}f''_a(\boldsymbol{q},\boldsymbol{q}')$ comes from the processes of inelastic and diffuse scattering by *the same* atom [10], so that for example the effect of correlations of thermal displacements of individual atoms does not contribute substantially to the result (1). It is sometimes difficult to establish the conditions of validity of the latter approximation quantitatively, although the analysis performed by Hall [38] suggests that the values of the Fourier components of the optical potential evaluated using the Einstein model appear to be reliable in most cases.

The real part of the amplitude $f'_a(\boldsymbol{q}-\boldsymbol{q}')$ is directly related to the Fourier transform of the electrostatic potential ϕ_a due to the nucleus and electrons of the atom,

$$f'_a(\boldsymbol{q}-\boldsymbol{q}') = -\frac{m}{2\pi\hbar^2}e\phi_a(\boldsymbol{q}-\boldsymbol{q}'), \tag{2}$$

and is proportional to the form factor for elastic scattering $f^{\mathrm{e}}(s)$, which is tabulated in the International Tables [39], as

$$f'_a(\boldsymbol{q}-\boldsymbol{q}') = \gamma f^{\mathrm{e}}_a(s), \tag{3}$$

where $s = |\boldsymbol{q} - \boldsymbol{q}'|/4\pi$ and $\gamma = m/m_0$, where m_0 is the electron rest mass.

The imaginary part of the amplitude $f''_a(\boldsymbol{q}, \boldsymbol{q}')$, which is associated with thermal motion of the atom, is related to the real part $f'_a(\boldsymbol{q}, \boldsymbol{q}')$ via the equation

$$f''_a(\boldsymbol{q}, \boldsymbol{q}') = \frac{1}{2\pi} \int \mathrm{d}^3 Q f'_a(\boldsymbol{q} - \boldsymbol{Q}) f'_a(\boldsymbol{Q} - \boldsymbol{q}') \delta(\boldsymbol{Q}^2 - k^2) \times \{1 - \exp[M_a(\boldsymbol{q} - \boldsymbol{q}') - M_a(\boldsymbol{q} - \boldsymbol{Q}) - M_a(\boldsymbol{Q} - \boldsymbol{q}')]\}. \tag{4}$$

For $\boldsymbol{q} = \boldsymbol{q}'$ Eq. (4) represents the optical theorem for electron scattering by an atom in a crystal. Using the variable s, and defining $f_a^{(\mathrm{TDS})}(s) = (\gamma)^{-1} f''_a(\boldsymbol{q}, \boldsymbol{q}')$, Eq. (4) can be transformed as

$$f_a^{(\mathrm{TDS})}(s) = \frac{4\pi\hbar}{m_0 v} \int \mathrm{d}^2 s' f_a^{\mathrm{e}}\left(\left|\frac{\boldsymbol{s}}{2} + \boldsymbol{s}'\right|\right) f_a^{\mathrm{e}}\left(\left|\frac{\boldsymbol{s}}{2} - \boldsymbol{s}'\right|\right) \{1 - \exp[-2B(s'^2 - s^2/4)]\}, \tag{5}$$

where $B = 8\pi^2 \langle u^2 \rangle$. This definition for $f_a^{(\mathrm{TDS})}(s)$ had been introduced by Bird and King (see formula (5b) of the paper [14]), who then evaluated the integral (5) numerically for a number of points and wrote a program to interpolate between these points, which is commonly used nowadays for calculation of the imaginary part of the scattering amplitude in k-space [10,26].

At first glance it might seem that in order to extend the Doyle–Turner approach to the case where the amplitude of scattering is complex it is sufficient to represent the imaginary part of the amplitude (5) by a set of a few Gaussian terms (historically the first attempt at approximating the imaginary part of the potential by a single Gaussian term was made by Ichimiya and Lehmpfuhl [40]). However as analysis shows, formula (5) has to be modified in order to make the fitting procedure convergent. Indeed, as follows from (5), in the limit of large s the magnitude of $f_a^{(\mathrm{TDS})}(s)$ increases exponentially as $f_a^{(\mathrm{TDS})}(s) \sim -\exp(Bs^2/2)$ and the relevant DT coefficients appear to be strongly dependent on the choice of the upper limit of the interval in which the fitting is performed. In order to remove the difficulty associated with exponential growth of the amplitude $f_a^{(\mathrm{TDS})}(s)$ at large s, we consider the quantity $f_a^{(\mathrm{TDS})}(s) \exp(-Bs^2/2)$ which vanishes in the limit $s \to \infty$. The problem of finding the DT representation of the crystal potential is then equivalent to the problem of finding the coefficients $\{a_n\}$ and $\{b_n\}$ in the following two expansions

$$f^{\mathrm{e}}(s) = \sum_{n=1}^{N} a_n^{(\mathrm{Re})} \exp(-b_n^{(\mathrm{Re})} s^2), \tag{6}$$

and

$$f^{(\mathrm{TDS})}(s) \exp(-Bs^2/2) = \sum_{n=1}^{N} a_n^{(\mathrm{TDS})} \exp(-b_n^{(\mathrm{TDS})} s^2). \tag{7}$$

Taking the Fourier transform of Eq. (1), and using (6) and (7), we obtain the real space representation of the optical potential of the crystal in the form

$$U(\boldsymbol{r}) = -\frac{2\pi\hbar^2}{m_0} \sum_a \sum_{n=1}^{N} a_n^{(\mathrm{Re})} \left(\frac{4\pi}{b_n^{(\mathrm{Re})} + B}\right)^{3/2} \exp[-4\pi^2 (\boldsymbol{r} - \boldsymbol{R}_a)^2 / (b_n^{(\mathrm{Re})} + B)] - \mathrm{i}\frac{2\pi\hbar^2}{m_0} \sum_a \sum_{n=1}^{N} a_n^{(\mathrm{TDS})} \left(\frac{4\pi}{b_n^{(\mathrm{TDS})} + B/2}\right)^{3/2} \exp[-4\pi^2 (\boldsymbol{r} - \boldsymbol{R}_a)^2 / (b_n^{(\mathrm{TDS})} + B/2)]. \tag{8}$$

To carry out RHEED computations one needs to evaluate the two-dimensional Fourier transform of the potential (8). The corresponding expression has the form

$$U_g(z) = -\frac{2\pi\hbar^2}{m_0 S_{\|}} \sum_{\alpha} \sum_{n=1}^{N} a_n^{(\mathrm{Re})} \sqrt{\frac{4\pi}{b_n^{(\mathrm{Re})} + B}} \exp[-i\boldsymbol{g}\cdot\boldsymbol{R}_{\|_\alpha}]$$
$$\times \exp[-\boldsymbol{g}^2(b_n^{(\mathrm{Re})} + B)/16\pi^2] \exp[-4\pi^2(z - Z_\alpha)^2/(b_n^{(\mathrm{Re})} + B)]$$
$$-i\frac{2\pi\hbar^2}{m_0 S_{\|}} \sum_{\alpha} \sum_{n=1}^{N} a_n^{(\mathrm{TDS})} \sqrt{\frac{4\pi}{(b_n^{(\mathrm{TDS})} + B/2)}} \exp[-i\boldsymbol{g}\cdot\boldsymbol{R}_{\|_\alpha}]$$
$$\times \exp[-\boldsymbol{g}^2(b_n^{(\mathrm{TDS})} + B/2)/16\pi^2] \exp[-4\pi^2(z - Z_\alpha)^2/(b_n^{(\mathrm{TDS})} + B/2)], \quad (9)$$

where $\boldsymbol{g}$ denotes a two-dimensional reciprocal lattice vector parallel to the surface, summation over α is carried out over the atoms belonging to a surface unit cell, $\boldsymbol{R}_{\|_\alpha}$ and Z_α denote the surface-parallel and normal components of the position vector of atom α in the cell and $S_{\|}$ denotes the area of the cell. The numerical value of the constant $2\pi\hbar^2/m_0$ entering (9) is 47.87798 Å^2 eV.

The numerical procedure of evaluation of the Doyle–Turner coefficients $\{a_n^{(\mathrm{TDS})}\}$ and $\{b_n^{(\mathrm{TDS})}\}$ includes two steps. In the first, the values of $f_a^{(\mathrm{TDS})}(s)$ were computed for 151 equally spaced points for all elements listed in the Tables (see below) in the interval $0 < s < 15$ Å^{-1}. In the second, the product $f_a^{(\mathrm{TDS})}(s)\exp(-Bs^2/2)$ was approximated by a set of $N = 5$ Gaussian terms using the Levenberg–Marquardt algorithm described in Refs. [41]. As a reference, for each element a set of five DT coefficients has also been determined for the real part of the amplitude of scattering. These coefficients are summarized in Tables 1 and 2. The fitting has been performed using 501 points in the interval $0 < s < 5$ Å^{-1}. The coefficients of the DT expansion representing the imaginary part of the amplitude are listed in Tables 3 and 4 for $E = 100$ keV and for the same set of values of the Debye–Waller factors B as that used by Radi [37]. It should be emphasized that although, according to Radi [37], the values of B quoted in Tables 3–4 correspond to room temperature $T = 293$ K, they may disagree with the results of more recent experimental measurements. In this case the sets of the DT coefficients $a_n^{(\mathrm{TDS})}$ and $b_n^{(\mathrm{TDS})}$ listed in Tables 3–4 should be considered as a starting approximation for further fitting using the Levenberg–Marquardt algorithm (see below).

As follows from Eq. (5), the coefficients $a_n^{(\mathrm{TDS})}$ are inversely proportional to the velocity of the electron, and this can be used to evaluate these coefficients for any energy within the range of validity of the Born approximation for electron-atom scattering. The accuracy of the DT representation thus obtained has been verified by comparing the results with the output of the program provided by Bird and King [14]. Good agreement was found for all values listed in Tables 1–4.

3. Results and discussion

In the previous section we showed how both the real and imaginary part of the potential can be represented in the DT form, which is consistent with the k-space calculations [14,15]. In this section we discuss the implications which these results may have for evaluation of the RHEED intensities.

We start from comparison of the *shape* of the imaginary part of the potential as calculated using the DT expansion and evaluated using the "proportional" model. Fig. 1 shows the dependence of the zero-order Fourier component of the optical potential ($\boldsymbol{g} = 0$ in Eq. (9)) which is calculated for the Ag(100) surface at room temperature for $E = 20$ keV. The value of the *constant* used in the "proportional" model is chosen in such a way that the average rate of absorption (which is proportional to the imaginary part of the amplitude of scattering through zero angle $f^{(\mathrm{TDS})}(0)$) is the same for both models. Fig. 1 shows that the imaginary part of the potential associated with thermal vibrations of atoms is strongly localized in the vicinity of the centres of atomic planes, whereas the "proportional" model gives rise to a broader imaginary part which is spread over the entire unit cell. In order to understand the origin of this difference, in Figs. 2 and 3 we have plotted the dependence of the real and imaginary parts of the effective amplitudes of scattering on s (the definition of

Table 1
The Doyle–Turner coefficients for the real part of the amplitude of scattering

Element	$a_1^{(Re)}$ (Å)	$a_2^{(Re)}$ (Å)	$a_3^{(Re)}$ (Å)	$a_4^{(Re)}$ (Å)	$a_5^{(Re)}$ (Å)	Abs. error
Li	0.1419E+01	0.1336E+01	0.3688E+00	0.1357E+00	0.2376E−01	0.1644E−03
Be	0.1112E+01	0.1375E+01	0.4087E+00	0.1285E+00	0.2562E−01	0.8932E−04
C	0.6617E+00	0.1193E+01	0.4899E+00	0.1316E+00	0.3083E−01	0.6470E−04
O	0.4552E+00	0.9158E+00	0.4525E+00	0.1258E+00	0.3311E−01	0.3264E−04
Na	0.2018E+01	0.1419E+01	0.8736E+00	0.3901E+00	0.6940E−01	0.7268E−03
Mg	0.2056E+01	0.1899E+01	0.8117E+00	0.3656E+00	0.6979E−01	0.5207E−03
Al	0.2023E+01	0.2526E+01	0.8571E+00	0.3998E+00	0.7571E−01	0.6943E−03
Si	0.1876E+01	0.2617E+01	0.8604E+00	0.3903E+00	0.7769E−01	0.5067E−03
K	0.3640E+01	0.2363E+01	0.2250E+01	0.5906E+00	0.1240E+00	0.3468E−02
Ca	0.4051E+01	0.3030E+01	0.2122E+01	0.5720E+00	0.1245E+00	0.2636E−02
Ti	0.3275E+01	0.2836E+01	0.1972E+01	0.5543E+00	0.1260E+00	0.2059E−02
V	0.2998E+01	0.2708E+01	0.1911E+01	0.5494E+00	0.1270E+00	0.1822E−02
Cr	0.2149E+01	0.2271E+01	0.1864E+01	0.5508E+00	0.1224E+00	0.1579E−02
Mn	0.2552E+01	0.2453E+01	0.1801E+01	0.5578E+00	0.1324E+00	0.1556E−02
Fe	0.2377E+01	0.2337E+01	0.1748E+01	0.5600E+00	0.1332E+00	0.1438E−02
Co	0.2198E+01	0.2238E+01	0.1707E+01	0.5662E+00	0.1356E+00	0.1330E−02
Ni	0.2120E+01	0.2098E+01	0.1642E+01	0.5578E+00	0.1364E+00	0.3189E−02
Cu	0.1477E+01	0.1780E+01	0.1617E+01	0.5787E+00	0.1393E+00	0.1171E−02
Zn	0.1838E+01	0.1938E+01	0.1560E+01	0.5784E+00	0.1409E+00	0.1007E−02
Ga	0.2131E+01	0.2513E+01	0.1605E+01	0.6912E+00	0.1568E+00	0.1757E−02
Ge	0.2259E+01	0.2746E+01	0.1533E+01	0.6738E+00	0.1563E+00	0.1432E−02
As	0.2237E+01	0.2839E+01	0.1445E+01	0.6379E+00	0.1536E+00	0.1073E−02
Rb	0.4404E+01	0.3344E+01	0.2699E+01	0.1088E+01	0.2180E+00	0.7246E−02
Sr	0.5231E+01	0.3809E+01	0.2760E+01	0.1068E+01	0.2199E+00	0.6075E−02
Y	0.4696E+01	0.3997E+01	0.2719E+01	0.1031E+01	0.2211E+00	0.5195E−02
Zr	0.4251E+01	0.4019E+01	0.2670E+01	0.9914E+00	0.2183E+00	0.4434E−02
Nb	0.3103E+01	0.3779E+01	0.2614E+01	0.9519E+00	0.2155E+00	0.3715E−02
Mo	0.2808E+01	0.3698E+01	0.2597E+01	0.9267E+00	0.2148E+00	0.3200E−02
Ru	0.2355E+01	0.3488E+01	0.2598E+01	0.8855E+00	0.2167E+00	0.2811E−02
Rh	0.2184E+01	0.3367E+01	0.2598E+01	0.8630E+00	0.2163E+00	0.2551E−02
Pd	0.1528E+01	0.3165E+01	0.1973E+01	0.7142E+00	0.1934E+00	0.9113E−03
Ag	0.1902E+01	0.3116E+01	0.2590E+01	0.8331E+00	0.2168E+00	0.2229E−02
Cd	0.2424E+01	0.3150E+01	0.2602E+01	0.8255E+00	0.2189E+00	0.2176E−02
Sn	0.3252E+01	0.3695E+01	0.2775E+01	0.8868E+00	0.2357E+00	0.3746E−02
Cs	0.5752E+01	0.5524E+01	0.3445E+01	0.1426E+01	0.3164E+00	0.1797E−01
Ba	0.7286E+01	0.5617E+01	0.3536E+01	0.1465E+01	0.3230E+00	0.1663E−01
La	0.6659E+01	0.5817E+01	0.3516E+01	0.1462E+01	0.3275E+00	0.1466E−01
Ce	0.6416E+01	0.5616E+01	0.3515E+01	0.1479E+01	0.3297E+00	0.1405E−01
Gd	0.5398E+01	0.4655E+01	0.3343E+01	0.1510E+01	0.3379E+00	0.1065E−01
Hf	0.4292E+01	0.4058E+01	0.2985E+01	0.1477E+01	0.3480E+00	0.6862E−02
Ta	0.3935E+01	0.4161E+01	0.2942E+01	0.1454E+01	0.3476E+00	0.6150E−02
W	0.3653E+01	0.4217E+01	0.2889E+01	0.1422E+01	0.3462E+00	0.5534E−02
Re	0.3442E+01	0.4241E+01	0.2834E+01	0.1386E+01	0.3441E+00	0.4790E−02
Os	0.3209E+01	0.4253E+01	0.2802E+01	0.1362E+01	0.3435E+00	0.4426E−02
Ir	0.2986E+01	0.4237E+01	0.2793E+01	0.1348E+01	0.3427E+00	0.3932E−02
Pt	0.2338E+01	0.4129E+01	0.2698E+01	0.1299E+01	0.3388E+00	0.3410E−02
Au	0.2193E+01	0.4083E+01	0.2672E+01	0.1275E+01	0.3380E+00	0.3031E−02
Tl	0.2811E+01	0.4293E+01	0.3207E+01	0.1415E+01	0.3649E+00	0.5031E−02
Pb	0.3202E+01	0.4427E+01	0.3196E+01	0.1392E+01	0.3651E+00	0.4712E−02
Th	0.6943E+01	0.7038E+01	0.3998E+01	0.1665E+01	0.4366E+00	0.1647E−01

Table 2
The Doyle–Turner coefficients for the real part of the amplitude of scattering

Element	$b_1^{(Re)}$ (Å^2)	$b_2^{(Re)}$ (Å^2)	$b_3^{(Re)}$ (Å^2)	$b_4^{(Re)}$ (Å^2)	$b_5^{(Re)}$ (Å^2)
Li	0.1155E+03	0.3643E+02	0.7008E+01	0.1114E+01	0.1113E+00
Be	0.6462E+02	0.2108E+02	0.4967E+01	0.8500E+00	0.9183E−01
C	0.3888E+02	0.1227E+02	0.3311E+01	0.6327E+00	0.7613E−01
O	0.2376E+02	0.7631E+01	0.2189E+01	0.4809E+00	0.6342E−01
Na	0.1162E+03	0.3083E+02	0.4674E+01	0.9460E+00	0.9264E−01
Mg	0.7816E+02	0.2323E+02	0.3988E+01	0.8278E+00	0.8588E−01
Al	0.7768E+02	0.2254E+02	0.4247E+01	0.8335E+00	0.8617E−01
Si	0.6211E+02	0.1868E+02	0.3935E+01	0.7690E+00	0.8234E−01
K	0.1471E+03	0.3008E+02	0.6125E+01	0.9463E+00	0.9584E−01
Ca	0.1064E+03	0.2827E+02	0.5388E+01	0.8847E+00	0.9168E−01
Ti	0.8682E+02	0.2248E+02	0.4435E+01	0.7933E+00	0.8525E−01
V	0.8061E+02	0.2058E+02	0.4085E+01	0.7569E+00	0.8259E−01
Cr	0.8282E+02	0.1815E+02	0.3796E+01	0.7132E+00	0.7775E−01
Mn	0.7131E+02	0.1789E+02	0.3595E+01	0.7177E+00	0.7965E−01
Fe	0.6752E+02	0.1678E+02	0.3380E+01	0.6930E+00	0.7752E−01
Co	0.6471E+02	0.1604E+02	0.3221E+01	0.6760E+00	0.7621E−01
Ni	0.5929E+02	0.1473E+02	0.2999E+01	0.6459E+00	0.7420E−01
Cu	0.6638E+02	0.1396E+02	0.2932E+01	0.6430E+00	0.7344E−01
Zn	0.5626E+02	0.1373E+02	0.2785E+01	0.6227E+00	0.7199E−01
Ga	0.6959E+02	0.1741E+02	0.3170E+01	0.7043E+00	0.7691E−01
Ge	0.5883E+02	0.1588E+02	0.2957E+01	0.6679E+00	0.7455E−01
As	0.4764E+02	0.1382E+02	0.2673E+01	0.6198E+00	0.7145E−01
Rb	0.1525E+03	0.2592E+02	0.5907E+01	0.9003E+00	0.8880E−01
Sr	0.1144E+03	0.2666E+02	0.5659E+01	0.8699E+00	0.8721E−01
Y	0.9910E+02	0.2430E+02	0.5246E+01	0.8309E+00	0.8530E−01
Zr	0.8883E+02	0.2185E+02	0.4842E+01	0.7841E+00	0.8247E−01
Nb	0.8391E+02	0.1891E+02	0.4471E+01	0.7402E+00	0.7974E−01
Mo	0.7844E+02	0.1749E+02	0.4214E+01	0.7097E+00	0.7782E−01
Ru	0.7146E+02	0.1540E+02	0.3809E+01	0.6619E+00	0.7516E−01
Rh	0.6877E+02	0.1452E+02	0.3620E+01	0.6362E+00	0.7356E−01
Pd	0.3578E+02	0.9358E+01	0.2649E+01	0.5205E+00	0.6525E−01
Ag	0.6488E+02	0.1311E+02	0.3309E+01	0.5990E+00	0.7100E−01
Cd	0.5815E+02	0.1309E+02	0.3198E+01	0.5871E+00	0.7031E−01
Sn	0.6148E+02	0.1555E+02	0.3300E+01	0.6177E+00	0.7252E−01
Cs	0.1650E+03	0.2347E+02	0.4882E+01	0.8986E+00	0.8763E−01
Ba	0.1254E+03	0.2359E+02	0.4966E+01	0.9067E+00	0.8784E−01
La	0.1094E+03	0.2250E+02	0.4840E+01	0.8947E+00	0.8726E−01
Ce	0.1071E+03	0.2210E+02	0.4784E+01	0.8868E+00	0.8652E−01
Gd	0.9478E+02	0.1985E+02	0.4273E+01	0.8116E+00	0.8130E−01
Hf	0.7404E+02	0.1688E+02	0.3590E+01	0.7097E+00	0.7514E−01
Ta	0.6831E+02	0.1602E+02	0.3473E+01	0.6917E+00	0.7411E−01
W	0.6344E+02	0.1502E+02	0.3331E+01	0.6704E+00	0.7291E−01
Re	0.5858E+02	0.1400E+02	0.3184E+01	0.6481E+00	0.7163E−01
Os	0.5506E+02	0.1324E+02	0.3080E+01	0.6311E+00	0.7065E−01
Ir	0.5232E+02	0.1266E+02	0.3013E+01	0.6176E+00	0.6971E−01
Pt	0.4816E+02	0.1136E+02	0.2828E+01	0.5918E+00	0.6816E−01
Au	0.4542E+02	0.1074E+02	0.2737E+01	0.5761E+00	0.6723E−01
Tl	0.6161E+02	0.1380E+02	0.3253E+01	0.6237E+00	0.7046E−01
Pb	0.5637E+02	0.1356E+02	0.3155E+01	0.6099E+00	0.6971E−01
Th	0.8675E+02	0.1871E+02	0.3821E+01	0.6940E+00	0.7551E−01

Table 3
The Doyle–Turner coefficients for the imaginary part of the amplitude for $T = 293$ K

Element	$a_1^{(TDS)}$ (Å)	$a_2^{(TDS)}$ (Å)	$a_3^{(TDS)}$ (Å)	$a_4^{(TDS)}$ (Å)	$a_5^{(TDS)}$ (Å)	Abs. error
Li	0.1410E−02	0.2365E−02	0.7757E−02	−0.1195E−02	−0.1245E−03	0.8971E−10
Be	0.9243E−03	0.1514E−02	0.2563E−02	−0.3810E−03	−0.1643E−04	0.6099E−09
C	0.6430E−03	0.1191E−02	0.1560E−02	0.2334E−02	−0.3732E−03	0.9525E−09
O	0.2787E−02	0.5258E−02	0.6952E−02	−0.1228E−02	−0.8000E−04	0.9820E−09
Na	0.1938E−02	0.9270E−02	0.9557E−01	−0.1368E−01	−0.1369E−02	0.1096E−07
Mg	0.3559E−02	0.1753E−01	0.5329E−01	−0.9258E−02	−0.6666E−03	0.6633E−08
Al	0.4680E−02	0.1827E−01	0.4113E−01	−0.7009E−02	−0.4708E−03	0.1067E−07
Si	0.4376E−02	0.1596E−01	0.2415E−01	−0.4068E−02	−0.2480E−03	0.2457E−07
K	0.3649E−02	0.6464E−01	0.2480E+00	−0.3846E−01	−0.3657E−02	0.8765E−07
Ca	0.8854E−02	0.6607E−01	0.1342E+00	−0.2261E−01	−0.1926E−02	0.6656E−07
Ti	0.1211E−01	0.4142E−01	0.7475E−01	−0.1207E−01	−0.8047E−03	0.1119E−06
V	0.1174E−01	0.5077E−01	0.8829E−01	−0.1471E−01	−0.1046E−02	0.9163E−07
Cr	0.1686E−01	0.3973E−01	0.6146E−01	−0.1096E−01	−0.8113E−03	0.1050E−06
Mn	0.1259E−01	0.5159E−01	0.8331E−01	−0.1429E−01	−0.1036E−02	0.9450E−07
Fe	0.1304E−01	0.5128E−01	0.8074E−01	−0.1391E−01	−0.1013E−02	0.1019E−06
Co	0.1312E−01	0.5618E−01	0.8691E−01	−0.1535E−01	−0.1154E−02	0.8939E−07
Ni	0.1301E−01	0.5625E−01	0.8642E−01	−0.1527E−01	−0.1153E−02	0.9317E−07
Cu	0.1287E−01	0.7642E−01	0.1180E+00	−0.2253E−01	−0.1801E−02	0.5594E−07
Zn	0.1007E−01	0.9275E−01	0.1772E+00	−0.3296E−01	−0.2653E−02	0.9429E−07
Ga	0.1104E−01	0.8868E−01	0.1522E+00	−0.2816E−01	−0.2215E−02	0.1103E−06
Ge	0.1242E−01	0.9287E−01	0.1772E+00	−0.3222E−01	−0.2533E−02	0.1343E−06
As	0.1467E−01	0.9454E−01	0.1817E+00	−0.3308E−01	−0.2603E−02	0.1413E−06
Rb	0.8999E−01	0.8257E+00	−0.9235E−01	−0.1924E−01	−0.1428E−02	0.4729E−06
Sr	0.1972E−01	0.1107E+00	0.4333E+00	−0.6762E−01	−0.5542E−02	0.4520E−06
Y	0.2607E−01	0.9737E−01	0.1827E+00	−0.3249E−01	−0.2522E−02	0.4502E−06
Zr	0.3116E−01	0.1041E+00	0.2219E+00	−0.3863E−01	−0.2989E−02	0.5199E−06
Nb	0.3639E−01	0.1089E+00	0.2479E+00	−0.4317E−01	−0.3402E−02	0.4185E−06
Mo	0.2725E−01	0.8550E−01	0.1465E+00	−0.2560E−01	−0.1955E−02	0.4062E−06
Ru	0.2770E−01	0.7727E−01	0.1323E+00	−0.2234E−01	−0.1379E−02	0.5427E−06
Rh	0.3717E−01	0.9695E−01	0.1806E+00	−0.3215E−01	−0.2593E−02	0.4027E−06
Pd	0.4845E−01	0.1164E+00	0.2450E+00	−0.4442E−01	−0.3674E−02	0.2825E−06
Ag	0.4650E−01	0.1425E+00	0.3422E+00	−0.5873E−01	−0.4915E−02	0.4029E−06
Cd	0.2159E−01	0.2208E+00	0.5872E+00	−0.9700E−01	−0.9251E−02	0.9055E−06
Sn	0.4279E−01	0.1304E+00	0.2703E+00	−0.4591E−01	−0.3653E−02	0.8584E−06
Cs	0.1381E+00	0.1697E+01	−0.1848E+00	−0.4414E−01	−0.3994E−02	0.3958E−06
Ba	0.4961E−01	0.2641E+00	0.8073E+00	−0.1295E+00	−0.1136E−01	0.1897E−05
La	0.5553E−01	0.2690E+00	0.6709E+00	−0.1109E+00	−0.9869E−02	0.1705E−05
Ce	0.5564E−01	0.2749E+00	0.7275E+00	−0.1195E+00	−0.1060E−01	0.1805E−05
Gd	0.5279E−01	0.2909E+00	0.6596E+00	−0.1136E+00	−0.9834E−02	0.1732E−05
Hf	0.4687E−01	0.2655E+00	0.4781E+00	−0.8683E−01	−0.7716E−02	0.1234E−05
Ta	0.4741E−01	0.2610E+00	0.4714E+00	−0.8507E−01	−0.7571E−02	0.1269E−05
W	0.3467E−01	0.1775E+00	0.2189E+00	0.1268E+00	−0.4894E−01	0.2141E−04
Re	0.5382E−01	0.2849E+00	0.5375E+00	−0.9800E−01	−0.8742E−02	0.1312E−05
Os	0.5030E−01	0.2451E+00	0.4492E+00	−0.7922E−01	−0.6947E−02	0.1549E−05
Ir	0.4942E−01	0.2206E+00	0.3983E+00	−0.6832E−01	−0.5486E−02	0.2110E−05
Pt	0.5924E−01	0.2717E+00	0.5077E+00	−0.9226E−01	−0.8379E−02	0.1081E−05
Au	0.7719E−01	0.3322E+00	0.7657E+00	−0.1376E+00	−0.1225E−01	0.1946E−05
Tl	0.3608E−01	0.3462E+00	0.1545E+01	−0.2323E+00	−0.2194E−01	0.5679E−05
Pb	0.2254E−01	0.3383E+00	0.1880E+01	−0.2606E+00	−0.2647E−01	0.8616E−05
Th	0.8368E−01	0.3882E+00	0.1024E+01	−0.1662E+00	−0.1465E−01	0.5784E−05

Table 4
The Doyle–Turner coefficients for the imaginary part of the amplitude for $T = 293$ K

Element	B (Å^2)	$b_1^{(TDS)}$ (Å^2)	$b_2^{(TDS)}$ (Å^2)	$b_3^{(TDS)}$ (Å^2)	$b_4^{(TDS)}$ (Å^2)	$b_5^{(TDS)}$ (Å^2)
Li	4.4374	0.4134E+02	0.1239E+02	0.3458E+01	0.7438E+00	0.1606E+00
Be	0.3869	0.1229E+02	0.1806E+01	0.4281E+00	0.6986E−01	0.1227E−01
C	0.1579	0.8264E+01	0.2448E+01	0.6204E+00	0.1802E+00	0.2571E−01
O	0.3000	0.4261E+01	0.1208E+01	0.3066E+00	0.5957E−01	0.1244E−01
Na	5.7323	0.4754E+02	0.1151E+02	0.3969E+01	0.8390E+00	0.1795E+00
Mg	1.4607	0.1977E+02	0.3499E+01	0.1245E+01	0.2706E+00	0.5394E−01
Al	0.8290	0.1446E+02	0.2357E+01	0.7672E+00	0.1563E+00	0.3086E−01
Si	0.3553	0.9058E+01	0.1293E+01	0.3574E+00	0.6746E−01	0.1353E−01
K	5.5665	0.5441E+02	0.1032E+02	0.4112E+01	0.9118E+00	0.1700E+00
Ca	1.6818	0.2168E+02	0.4563E+01	0.1380E+01	0.2971E+00	0.5970E−01
Ti	0.5132	0.7653E+01	0.1928E+01	0.4868E+00	0.9341E−01	0.1865E−01
V	0.5922	0.8186E+01	0.2075E+01	0.5453E+00	0.1088E+00	0.2192E−01
Cr	0.3553	0.4341E+01	0.1169E+01	0.3356E+00	0.6877E−01	0.1452E−01
Mn	0.4501	0.6122E+01	0.1591E+01	0.4187E+00	0.8484E−01	0.1756E−01
Fe	0.3948	0.5309E+01	0.1405E+01	0.3711E+00	0.7505E−01	0.1570E−01
Co	0.4027	0.5126E+01	0.1373E+01	0.3732E+00	0.7739E−01	0.1631E−01
Ni	0.3632	0.4663E+01	0.1257E+01	0.3393E+00	0.7025E−01	0.1497E−01
Cu	0.5448	0.5072E+01	0.1490E+01	0.4749E+00	0.1062E+00	0.2210E−01
Zn	0.8685	0.8138E+01	0.2010E+01	0.7303E+00	0.1640E+00	0.3310E−01
Ga	0.6396	0.7598E+01	0.1654E+01	0.5537E+00	0.1216E+00	0.2488E−01
Ge	0.7185	0.8827E+01	0.1774E+01	0.6171E+00	0.1350E+00	0.2739E−01
As	0.6869	0.8518E+01	0.1694E+01	0.5901E+00	0.1293E+00	0.2630E−01
Rb	8.5826	0.1719E+02	0.5597E+01	0.1286E+01	0.3423E+00	0.6505E−01
Sr	1.6502	0.1716E+02	0.4301E+01	0.1292E+01	0.2742E+00	0.5379E−01
Y	0.4343	0.6557E+01	0.1237E+01	0.3874E+00	0.8246E−01	0.1737E−01
Zr	0.5290	0.6896E+01	0.1434E+01	0.4641E+00	0.9831E−01	0.2032E−01
Nb	0.5843	0.6515E+01	0.1522E+01	0.5046E+00	0.1080E+00	0.2226E−01
Mo	0.2606	0.4605E+01	0.8710E+00	0.2459E+00	0.5062E−01	0.1110E−01
Ru	0.1974	0.3793E+01	0.7254E+00	0.1950E+00	0.3754E−01	0.7456E−02
Rh	0.2921	0.4092E+01	0.9019E+00	0.2681E+00	0.5704E−01	0.1265E−01
Pd	0.4343	0.4275E+01	0.1163E+01	0.3761E+00	0.8300E−01	0.1781E−01
Ag	0.6632	0.5391E+01	0.1760E+01	0.5561E+00	0.1206E+00	0.2496E−01
Cd	1.5791	0.1162E+02	0.3466E+01	0.1205E+01	0.2696E+00	0.5372E−01
Sn	0.3869	0.4640E+01	0.1223E+01	0.3462E+00	0.7220E−01	0.1546E−01
Cs	11.3698	0.2027E+02	0.7097E+01	0.1697E+01	0.5032E+00	0.9217E−01
Ba	1.6107	0.1442E+02	0.3581E+01	0.1259E+01	0.2731E+00	0.5232E−01
La	1.1449	0.1163E+02	0.2692E+01	0.9182E+00	0.1997E+00	0.3940E−01
Ce	1.2317	0.1178E+02	0.2831E+01	0.9831E+00	0.2139E+00	0.4184E−01
Gd	0.8133	0.8021E+01	0.1903E+01	0.6638E+00	0.1458E+00	0.2921E−01
Hf	0.3632	0.4628E+01	0.1023E+01	0.3115E+00	0.6971E−01	0.1528E−01
Ta	0.3395	0.4507E+01	0.9811E+00	0.2937E+00	0.6535E−01	0.1446E−01
W	0.1895	0.3829E+01	0.8004E+00	0.1958E+00	0.1958E+00	0.2732E−01
Re	0.3869	0.4728E+01	0.1038E+01	0.3274E+00	0.7388E−01	0.1610E−01
Os	0.2763	0.4024E+01	0.8609E+00	0.2462E+00	0.5339E−01	0.1205E−01
Ir	0.2211	0.3548E+01	0.7533E+00	0.2046E+00	0.4237E−01	0.9399E−02
Pt	0.3158	0.3999E+01	0.8964E+00	0.2727E+00	0.6131E−01	0.1376E−01
Au	0.5843	0.4933E+01	0.1301E+01	0.4709E+00	0.1069E+00	0.2223E−01
Tl	1.7134	0.1212E+02	0.3663E+01	0.1254E+01	0.2712E+00	0.5235E−01
Pb	2.5266	0.1936E+02	0.5163E+01	0.1781E+01	0.3724E+00	0.7127E−01
Th	0.6001	0.7462E+01	0.1594E+01	0.4908E+00	0.1045E+00	0.2161E−01

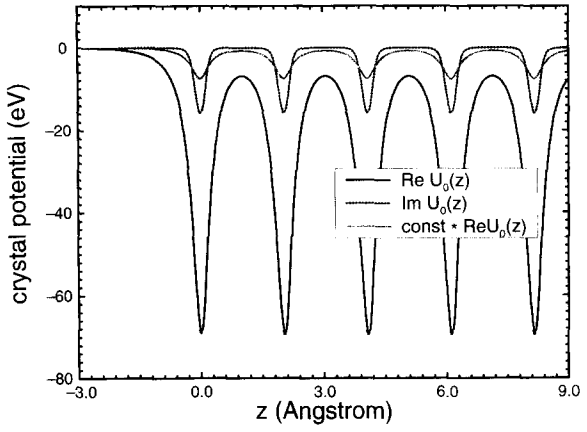

Fig. 1. The optical potential $U_0(z)$ calculated for the (100) face of Ag crystal for E = 20 keV using the DT coefficients taken from Tables 1–4 and the "proportional" model.

these amplitudes includes the Debye–Waller factor). It is evident from the comparison of the results shown in Figs. 2 and 3 that the imaginary part of the potential of a single atom is more delocalized in k-space than the corresponding real part, therefore implying stronger localization of the imaginary part near the atomic cores in real space. Furthermore we note that $F^{(\mathrm{TDS})}(s)$ becomes negative for large s. This is in agreement with the original considerations of Yoshioka and Kainuma [42], and later with those of Whelan [33], and Humphreys and Hirsch [43].

The next point to be analysed is whether the change in the *shape* of the imaginary part of the potential can affect considerably the position and height of the peaks in the RHEED rocking curves. In the past the problem of sensitivity of the RHEED rocking curves to the choice of the input parameters was mainly addressed as a question concerning the convergence of the computational procedure. Zhao, Poon and Tong [22] noted that the number of rods (in other words, the number of two-dimensional reciprocal lattice vectors $\boldsymbol{g}$) included in the computational scheme should be large enough in order to obtain a convergent result. Examination of the same problem performed later by Meyer-Ehmsen [24] showed that generally the conclusion made by Zhao, Poon and Tong [22] regarding the large number of rods to be used in calculations is correct, but in many cases

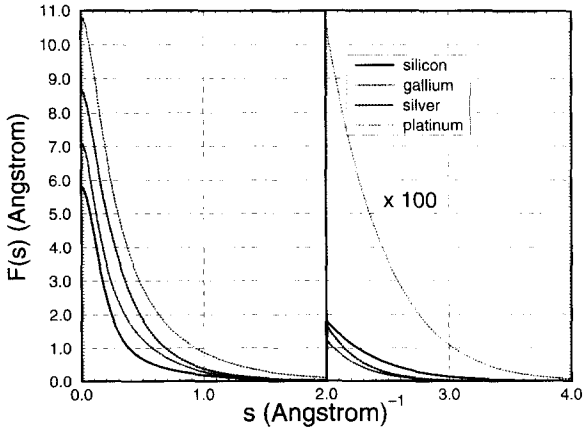

Fig. 2. The real part of the effective amplitude of scattering of electrons by atoms in a crystal. The definition of the amplitude includes the Debye–Waller factor $F(s) = f^e(s)\exp(-Bs^2)$. All the curves correspond to room temperature.

computations employing relatively few rods result in a rocking curve which does not differ much from the curve calculated using more rods. To the best of our knowledge however, the sensitivity of RHEED rocking curves to the choice of the *shape* of the imaginary part of the potential has not been considered in detail previously.

Therefore we have computed several RHEED rocking curves for the unreconstructed Ag(100) surface using different numbers of rods (21 and 51) and considering two models of absorption (the "proportional" model and the DT expansion based on the data presented in Tables 3 and 4). Computations have been performed on an Hewlett-Packard Apollo workstation using a multislice version of the R-matrix method. The dependence of the specular intensity on the angle of incidence is shown in Figs. 4 and 5. The solid curve shown in Fig. 4 agrees qualitatively with the results published by Zhao et al. [22] (who carried out calculations using the proportional model) and is found to be fully convergent with respect to the number of beams included. Examination of the other two curves in Fig. 4 shows that the intensity depends noticeably on the shape of the imaginary part of the potential and is less sensitive to many-beam effects than to the choice of the absorption potential (the *average* rate of absorption remained the same for all three curves shown in Fig. 4). Fig. 5 shows three curves computed for the same number of rods (51), but for varying magnitude of the *constant* used in the proportional model. Examination of Fig. 5 shows that by varying this *constant* it is possible to improve the agreement between the results calculated using the two different models of absorption. However, by changing the magnitude of the *constant* it was not possible to reproduce the two sharp peaks at $\zeta = 1.9°$ and $\zeta = 3.35°$.

It is known that there exists an additional contribution to the absorption which is associated with electronic excitations. This part of the absorption potential is delocalized in real space and, as was found by Zhao et al. [22], the presence of this "homogeneous" component of absorption does not appreciably affect the relative intensities of various peaks in the RHEED rocking curves.

In view of the results discussed above it is interesting to compare the absorption parameters obtained from k-space calculations with the data published recently by other authors [2,3,44]. McCoy et al. [2,3] and Ma et al. [44] discussed the application of RHEED to the problem of the determination of the structure of the GaAs(001) 2×4 surface, for which the experimental observations had been performed at $T = 838$ K. Fig. 6 shows the real and imaginary parts of the effective amplitudes of scattering for Ga and As atoms calculated for $T = 838$ K and $E = 12.5$ keV using the Debye–Waller factors $B_{Ga} = 1.772$ Å^2 and $B_{As} = 1.911$ Å^2 as given by Reid [45]. The curves depicted in Fig. 6 show that at high temperatures the imaginary part of the amplitude becomes more localized in k-space therefore making the "proportional" model more acceptable (this results from the relatively large amplitudes of thermal vibrations at $T = 838$ K $\sqrt{\langle u^2 \rangle}_{Ga} = 0.1498$ Å and

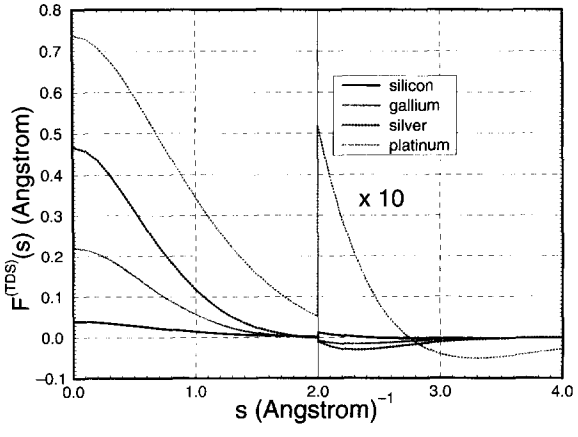

Fig. 3. The imaginary part of the effective amplitude of scattering of electrons by atoms in a crystal. The definition of the amplitude includes the Debye–Waller factor $F^{(TDS)}(s) = f^{(TDS)}(s)\exp(-Bs^2)$. All the curves correspond to room temperature.

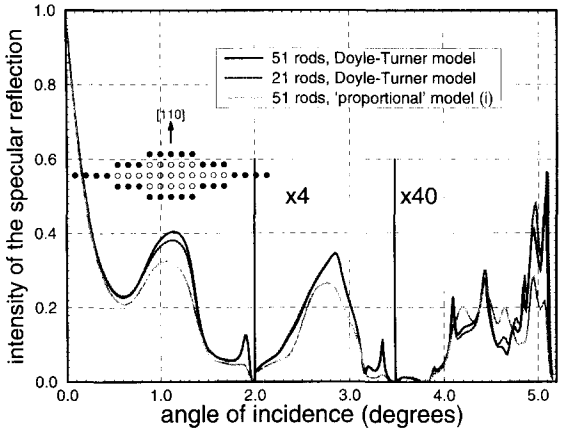

Fig. 4. The dependence of the intensity of the specular reflection on the angle of incidence calculated for 20 keV electrons incident on the Ag(100) surface along the ⟨110⟩ azimuth. Calculations have been performed for room temperature using the data from Tables 1–4. A schematic diagram representing the rods selected for the calculations is shown in the inset. The 21-rod calculation uses rods (perpendicular to the plane of the diagram) represented by open circles only. The value of the *constant* used in the "proportional" model (i) is chosen in such a way that the average rate of absorption is the same for all three curves shown in this figure.

$\sqrt{\langle u^2\rangle}_{As} = 0.1556$ Å, compared with $\sqrt{\langle u^2\rangle}_{Ga} = 0.0804$ Å and $\sqrt{\langle u^2\rangle}_{As} = 0.0896$ Å at $T = 295$ K).

The ratio $f^{(TDS)}(0)/f^{e}(0)$ for both Ga and As atoms is found to be almost the same and approximately equal to 0.13 (more precisely, $f^{(TDS)}_{Ga}(0)/f^{e}_{Ga}(0) = 0.128$ and $f^{(TDS)}_{As}(0)/f^{e}_{As}(0) = 0.134$). This number is about two times smaller than the value 0.237 determined by McCoy et al. [3] by fitting the experimental RHEED rocking curves to theoretical calculations. Ma et al. [44] analysing another set of experimental data obtained for the same surface concluded that the value 0.1 gives the best agreement between experimental data and theoretical calculations. This value agrees better with our estimate of 0.13. However in a paper published later, Lordi, Ma and Eades [13] used the same value 0.1 in order to simulate absorption in MgO at room temperature. According to the results shown in Figs. 2 and 3, a somewhat smaller value is likely to be expected

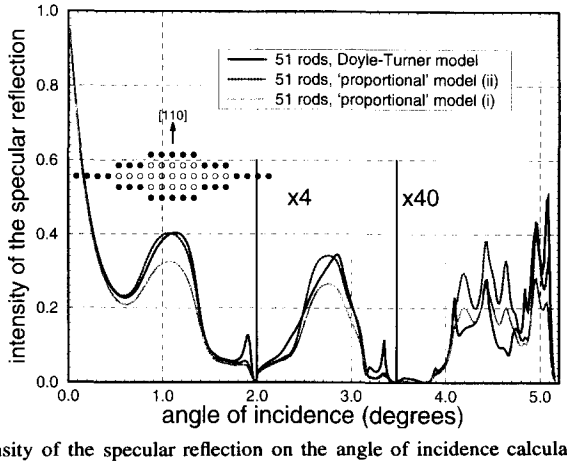

Fig. 5. The dependence of the intensity of the specular reflection on the angle of incidence calculated for 20 keV electrons incident on the Ag(100) surface along the ⟨110⟩ azimuth. Calculations have been performed for room temperature using the data from Tables 1–4. A schematic diagram representing the rods selected for the calculations is shown in the inset. The value of the *constant* used in the "proportional" model (ii) is chosen in such a way that the average rate of absorption is 20% lower than for two other curves shown in this figure.

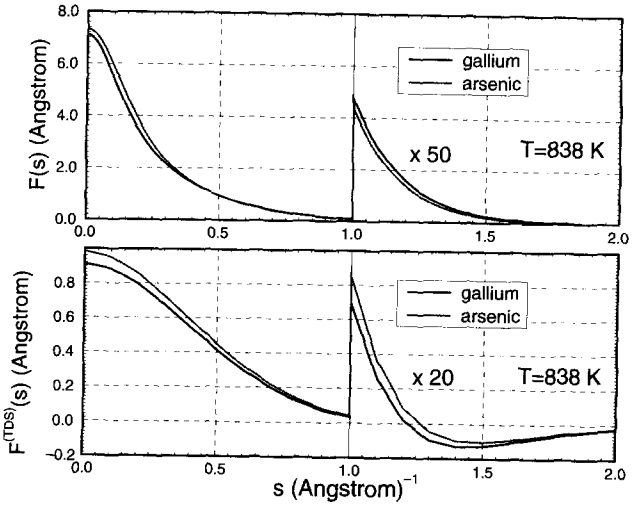

Fig. 6. Real and imaginary parts of the effective amplitudes of scattering of both types of atoms in a GaAs single crystal. The energy of the electrons is 12.5 keV.

in the latter case.

Therefore we can conclude that the absorption parameters used lately for carrying out RHEED calculations, or obtained as a result of fitting of computed rocking curves to experimental data generally do not agree very well both with the results of theoretical k-space calculations and with the data obtained from transmission electron diffraction experiments [37,14]. Two explanations of this are possible. The first is that even for a perfect surface the "proportional" model is not entirely consistent with the physical contents of the problem itself. Phonon scattering generally results in an imaginary part which is more localized around atomic cores than the effective absorption potential given by the "proportional" model. Implementation of the DT expansion proposed in the present paper can provide a more realistic representation of the imaginary part of the optical potential arising from this type of incoherent scattering. Electronic excitations results in an effective absorption potential which is delocalized in real space and therefore it cannot be included in the framework of the "proportional" model at all. It is possible that the effect of electronic excitations could be taken into consideration by introducing a separate input parameter in the RHEED computational scheme. If energy filtering is not employed for carrying out experimental observations, multiple scattering by electronic excitations and the resulting damping of coherence between various Bloch states may occur [46], which will require solving the kinetic equation for the density matrix [47]. Mathematical methods suitable for solving the kinetic equation in backscattering geometry have recently been developed by Dudarev, Rez and Whelan [48]. Another possible process of scattering is associated with the presence of surface disorder, which is known to result in strong diffuse scattering [49] and which leads to the appearance of an additional contribution to the optical potential localized near the surface [7,8,10]. This might explain the origin of the somewhat excessive value of the ratio of imaginary to real part of the potential found by McCoy et al. [2,3], although more careful analysis is required in order to identify all the possible processes of incoherent scattering affecting the experimentally observed RHEED patterns.

4. Availability of the computer program

The computer program which is described in this paper and which can be further used for evaluation of the Doyle–Turner coefficients both for the real and for the imaginary parts of atomic potentials of any

compound at any temperature, is freely available upon request to the interested reader. The program does not require linking to any of the existing standard computer library routines (e.g. NAG) and can be executed on a personal computer. The source file and the description of the program are available through e-mail from Dr. S. L. Dudarev (sergei.dudarev@materials.oxford.ac.uk) or from Professor M. J. Whelan, FRS (michael.whelan@materials.oxford.ac.uk)

Acknowledgements

We are grateful to the referee for pointing out that varying the *constant* in the proportional model can improve the agreement between the curves calculated using the two different models of absorption considered in this paper. S.L.D. acknowledges financial support of this work from the Engineering and Physical Science Research Council (EPSRC) (grant number GR/H96423). He is also grateful to Linacre College, Oxford, for the provision of a Research Fellowship. Numerical computations have been performed using the facilities of the Materials Modelling Laboratory, Department of Materials, University of Oxford, which is funded in part by the EPSRC (grant number GR/H58278).

References

[1] A. Ichimiya, Surf. Sci. 192 (1987) L893.
[2] J.M. McCoy, U. Korte, P.A. Maksym and G. Meyer-Ehmsen, Surf. Sci. 261 (1992) 29.
[3] J.M. McCoy, U. Korte, P.A. Maksym and G. Meyer-Ehmsen, Phys. Rev. B48 (1993) 4721.
[4] U. Korte and G. Meyer-Ehmsen, Surf. Sci. 271 (1992) 616.
[5] A. Ichimiya, S. Kohmoto, H. Nakahara and Y. Horio, Ultramicroscopy 48 (1993) 425.
[6] G. Lehmpfuhl, A. Ichimiya and H. Nakahara, Surf. Sci. 245 (1991) L159;
Y. Horio and A. Ichimiya, Ultramicroscopy 55 (1994) 321.
[7] S.L. Dudarev, D.D. Vvedensky and M.J. Whelan, Surf. Sci. 324 (1995) L355
[8] S.L. Dudarev, D.D. Vvedensky and M.J. Whelan, Phys. Rev. B 50 (1994) 14525.
[9] A. Howie and R.M. Stern, Z. Naturforsch. 27a (1972) 382.
[10] S.L. Dudarev, L.-M. Peng and M.J. Whelan, Surf. Sci. 279 (1992) 380
[11] J.C.H. Spence and J.M. Zuo, Electron Microdiffraction (Plenum, New York, 1992).
[12] J.C.H. Spence and J. Mayer, in: Proc. 49th Annual Meeting of EMSA, Eds. G.W. Bailey and E.L. Hall (San Francisco Press, San Francisco, 1991) p. 616.
[13] S. Lordi, Y. Ma and J.A. Eades, Ultramicroscopy 55 (1994) 284.
[14] D.M. Bird and Q.A. King, Acta Crystallogr. A 46 (1990) 202, and references therein.
[15] A. Weickenmeier and H. Kohl, Acta Crystallogr. A 47 (1991) 590.
[16] R. James, D.M. Bird and A.G. Wright, Acta Crystallogr. A 50 (1994) 357.
[17] M. Tournarie, Journ. Phys. Soc. Japan 17, Suppl. B-II (1962) 98.
[18] J.B. Pendry and P. Gard, J. Phys. C 8 (1975) 2048.
[19] P.A. Maksym and J.L. Beeby, Surf. Sci. 110 (1981) 423.
[20] A. Ichimiya, Japan. J. Appl. Phys. 22 (1983) 176.
[21] L.-M. Peng and J.M. Cowley, Acta Crystallogr. A 42 (1986) 545.
[22] T.C. Zhao, H.C. Poon and S.Y. Tong, Phys. Rev. B 38 (1988) 1172.
[23] L.D. Marks and Y. Ma, Acta Crystallogr. A 44 (1988) 392.
[24] G. Meyer-Ehmsen, Surf. Sci. 219 (1989) 177.
[25] Z. Mitura, M. Jalochowski and M. Subotowicz, Phys. Lett. A 150 (1990) 51.
[26] A.E. Smith and T.W. Josefsson, Ultramicroscopy 55 (1994) 247.
[27] P. Rez, Acta Crystallogr. A 51 (1995) 38
[28] L.-M. Peng and M.J. Whelan, Surf. Sci. 268 (1992) L325.
[29] G.H. Smith and R.E. Burge, Acta Crystallogr. 15 (1962) 182.
[30] P.A. Doyle and P.S. Turner, Acta Crystallogr. A 24 (1968) 390.
[31] D. Rez, P. Rez and I. Grant, Acta Crystallogr. A 50 (1994) 481.
[32] H. Hashimoto, A. Howie and M.J. Whelan, Proc. Roy. Soc. (London) A 269 (1962) 80.

[33] M.J. Whelan, J. Appl. Phys. 36 (1965) 2103.
[34] P. Rez, Ultramicroscopy 52 (1993) 260.
[35] C.J. Rossouw, P.R. Miller, J. Drennan and L.J. Allen, Ultramicroscopy 34 (1990) 149.
[36] D.M. Bird, Acta Crystallogr. A 46 (1990) 208.
[37] G. Radi, Acta Crystallogr. A 26 (1970) 41.
[38] C.R. Hall, Philos. Mag. 12 (1965) 815.
[39] *International Tables for X-ray Crystallography*, Vol IV, Eds. J.A. Ibers and W.C. Hamilton (Kynoch Press, Birmingham, 1974) p. 152.
[40] A. Ichimiya and G. Lehmpfuhl, Z. Naturforsch. 33a (1978) 269.
[41] W.H. Press, S.A. Teukolsky, W.A. Vetterling and B.A. Flannery, Numerical Recipes in FORTRAN, 2nd ed. (Cambridge University Press, Cambridge, 1992) p. 678.
[42] H. Yoshioka and Y. Kainuma, J. Phys. Soc. Jpn. 17, Suppl. B-II (1962) 134.
[43] C.J. Humphreys and P.B. Hirsch, Philos. Mag. 18 (1968) 115.
[44] Y. Ma, S. Lordi, P.K. Larsen and J.A. Eades, Surf. Sci. 289 (1993) 47.
[45] J.S. Reid, Acta Crystallogr. A 39 (1983) 1.
[46] S.L. Dudarev, L.-M. Peng and M.J. Whelan, Phys. Lett. A170 (1992) 111;
L.-M. Peng, S.L. Dudarev and M.J. Whelan, Phys. Lett. A 175 (1993) 465.
[47] S.L. Dudarev, L.-M. Peng and M.J. Whelan, Phys. Rev. B 48 (1993) 13408.
[48] S.L. Dudarev, P. Rez and M.J. Whelan, Phys. Rev. B 51 (1995) 3397.
[49] P.K. Larsen and G. Meyer-Ehmsen, Surf. Sci. 240 (1990) 168.